Available online at website: https://journal.bcrec.id/index.php/bcrec

Bulletin of Chemical Reaction Engineering & Catalysis, 21 (2) 2026, 262-273

Original Research Article

Synthesis of Cu-PTC (Perylene 3,4,9,10-tetracarboxylate) Metal-Organic Framework (MOF) for Methylene Blue Photodegradation

Farhah Syahidatul Mala[1], Nanda Saridewi[2,3*], Siti Nurbayti[1], A. Adawiah[1], Agustino Zulys[3]

[1]Department of Chemistry, Faculty of Science and Technology, UIN Syarif Hidayatullah Jakarta, Jl. Ir. H. Juanda No. 95 Ciputat Tangerang Selatan 15412, Indonesia.
[2]Department of Chemistry Education, Faculty of Tarbiya and Teaching Sciences, UIN Syarif Hidayatullah, Jl. Ir. H. Juanda No. 95 Ciputat Tangerang Selatan 15412, Indonesia.
[3]Department of Chemistry, Faculty of Mathematics and Natural Sciences, University of Indonesia, Jl. Lingkar Kampus Raya, Pondok Cina, Beji, Depok, Jawa Barat 16424, Indonesia.

Received: 31th October 2025; Revised: 20th January 2026; Accepted: 21st January 2026
Available online: 2nd February 2026; Published regularly: August 2026

Abstract

Disposal of synthetic dye waste, including methylene blue, has been increasing in recent years. The photocatalytic method is an effective approach for degrading dyes, using Metal–Organic Frameworks (MOFs) as catalysts and light as the energy source. This study aims to synthesize Cu-PTC MOF as a photocatalyst and evaluate its performance in degrading methylene blue dye. Cu-PTC was synthesized using $Cu(NO_3)_2.3H_2O$ and perylene-3,4,9,10-tetracarboxylic dianhydride (PTCDA) via a solvothermal method. The resulting MOF was characterized using X-ray Diffraction (XRD), Ultraviolet–Visible Diffuse Reflectance Spectroscopy (UV-Vis DRS), Fourier Transform Infrared Spectroscopy (FTIR), and Scanning Electron Microscopy (SEM). Cu-PTC exhibits a bandgap energy of 1.72 eV and characteristic functional groups at wavenumbers 1689 cm^{-1} (C=O), 1590 cm^{-1} and 1360 cm^{-1} (-COO), 3450 cm^{-1} (O-H), and 738 cm^{-1} and 654 cm^{-1} (Cu-O). The Cu-PTC MOF has a crystallinity degree of 85.35%, a crystal size of 35.33 nm, and a rod-like surface morphology. Under visible light irradiation, it achieves an optimum degradation efficiency of 71.45%, with an adsorption capacity of 73.28 mg/g for methylene blue dye at a concentration of 50 ppm, using 25 mg of Cu-PTC MOF at pH of 7 over a period of 60 minutes.

Keywords: Cu-PTC; methylene blue; photocatalyst; solvothermal; Metal-Organic Framework; MOF

How to Cite: Mala, F. S., Saridewi, N., Nurbayti, S., Adawiah, A., Zulys, A. (2026). Synthesis of Cu-PTC (Perylene 3,4,9,10-tetracarboxylate) Metal-Organic Framework (MOF) for Methylene Blue Photodegradation. *Bulletin of Chemical Reaction Engineering & Catalysis*, 21 (2), 262-273. (DOI: 10.9767/bcrec.20525)

Permalink/DOI: https://doi.org/10.9767/bcrec.20525

Supporting Information (SI): https://journal.bcrec.id/index.php/bcrec/article/downloadSuppFile/20525/5939

1. Introduction

Discharge of synthetic dye waste into water bodies has been increasing in recent years. This waste originates from various industries, including textiles, cosmetics, paper, and pharmaceuticals [1]. Numerous efforts have been made to remove organic dye pollutants from aqueous environments due to their harmful effects on aquatic life and human health. Their high stability, stemming from a high content of aromatic compounds, makes these dyes resistant to biological degradation [2]. Methylene blue is one such dye that is persistent in the environment and exhibits toxic, carcinogenic, and mutagenic properties [3].

Several methods have been developed to remove dye pollutants from water, such as electrochemical processes, biological technologies, coagulation, flocculation, ion exchange, membrane filtration, and reverse osmosis [4]. However, these methods have several limitations, including low removal efficiency, high cost, long processing times, high sludge production, suitability only for small-scale remediation, and

* Corresponding Author.
Email: nanda.saridewi@uinjkt.ac.id (N. Saridewi)

the generation of toxic by-products [5]. Advanced Oxidation Processes (AOPs) have been identified as a promising approach for degrading organic pollutants in water [6]. The key feature of AOPs is the in-situ generation of highly reactive oxidizing free radicals, particularly hydroxyl radicals (•OH). These reactive radicals can oxidize organic pollutants into CO_2, H_2O, or specific inorganic ions, thereby avoiding the formation of by-products that might hinder complete degradation of the target pollutants [7].

The photocatalytic system is a part of AOPs that is highly effective, cost-efficient, and environmentally friendly, making it a promising remediation approach. The photocatalytic process occurs in three main steps. First, when the photon energy matches the bandgap of the semiconductor photocatalyst, electron–hole pairs are generated (e^-–h^+). These charge carriers are then separated and transported to the surface of the photocatalyst. Finally, the light-induced charge carriers participate in redox reactions at the active sites on the photocatalyst surface [8].

In general, materials suitable for photocatalytic dye degradation are semiconductors, including Metal–Organic Frameworks (MOFs) [9]. Photocatalysis is typically carried out using semiconductor-based catalysts because they possess a relatively small bandgap energy. When illuminated by light (photons) with energy equal to or greater than this bandgap, the material can absorb the energy and excite electrons from the valence band to the conduction band. This electron transfer creates electron holes in the valence band, which play a key role in generating hydroxyl radicals that degrade dyes [10].

The use of MOFs as materials in photochemical reactions has been widely developed and represents a promising option for removing dye contaminants from wastewater [11]. MOFs possess characteristics well-suited for wastewater treatment, including a unique porous structure, tunable pore size, abundant adsorption sites, and high specific surface area and porosity [12,13]. MOFs are also promising materials for photocatalysis due to their tunable bandgap, which enables them to absorb light and generate the electron–hole pairs required for photocatalytic reactions [14].

One of the most used methods for synthesizing MOFs is the solvothermal method. This approach is widely employed because it is straightforward to carry out and can produce materials with high crystallinity [15]. The solvothermal method offers several advantages, including controllable particle size and morphology by varying the starting materials and reaction conditions, as well as producing MOFs with high reactivity [16].

Saridewi and her team studied Cr-PTC synthesized from chromium ions and perylene-3,4,9,10-tetracarboxylate ligand using the solvothermal method. The resulting material exhibited a bandgap energy of 2.01 eV. Cr-PTC effectively removed methylene blue pollutant (50 ppm) with an adsorption capacity of 87.22 mg/g within 180 minutes under visible light irradiation [17]. Perylene-3,4,9,10-tetracarboxylate can reduce the bandgap energy of MOFs due to the conjugated aromatic ring bonds, making it responsive to visible light [18].

Zhang and his team synthesized two 3D MOFs $[Cu(4,4'\text{-bipy})Cl]_n$ (MOF 1) and $[Co(4,4'\text{-bipy})(HCOO)_2]_n$ (MOF 2). MOF 1 achieved 93.93% degradation of methylene blue after 150 minutes under visible light, whereas MOF 2 reached only 54.70% degradation at the same time [19]. Copper-based MOFs exhibit high stability, abundant elemental availability, and high surface area and porosity [20], making copper a promising candidate for photocatalyst development.

Based on a literature review, no studies have been found on the combination of copper metal ions and PTC ligands in a MOF used as a photocatalyst for methylene blue degradation. The main objective of this study is to synthesize Cu-PTC MOF via the solvothermal method and evaluate its photocatalytic performance in degrading methylene blue under visible light irradiation. Additionally, the effects of methylene blue concentration, MOF dosage, and pH were also investigated.

2. Materials and Method

2.1. Materials

The materials used in this study included perylene 3,4,9,10-tetracarboxylic dianhydride (PTCDA) (Sigma Aldrich, 97%), copper (II) nitrate trihydrate ($Cu(NO_3)_2.3H_2O$) (Merck), distilled water, sodium hydroxide (NaOH), ethanol (96%), N, N-dimethylformamide (DMF) (Pallav), and methylene blue (Merck).

2.2. Conversion of PTCDA to Na_4PTC

A total of 500 mg (1.27 mmol) of PTCDA was dissolved in 50 mL of distilled water, followed by the addition of 356 mg of NaOH (8.9 mmol). The mixture was stirred at room temperature using a magnetic stirrer at 300 rpm for 1 hour. Excess ethanol was then added to the mixture to precipitate yellow Na_4PTC. The solid Na_4PTC was collected by filtration and washed repeatedly with ethanol until neutral pH was reached. The product was dried overnight at room temperature [17].

2.3. Synthesis of Cu-PTC MOF

Cu-PTC MOF was synthesized by dissolving Cu $(NO_3)_2.3H_2O$ (1 mmol) and Na_4PTC (0,5 mmol) in a mixture of 5 mL DMF and 25 mL deionized water. The solution was stirred thoroughly and then transferred into a Teflon-lined autoclave tube. The sealed autoclave was heated in an oven at 170 °C for 24 hours. After heating, the autoclave was allowed to cool naturally to room temperature over 24 hours. The resulting Cu-PTC solid was collected by filtration and washed repeatedly with deionized water until the filtrate became clear. The product was then dried overnight in an oven at 70 °C [17].

2.4. Characterizations

Analysis of diffraction patterns and crystal size using the Debye-Scherrer equation was performed using XRD (Rigaku Miniflex) with Cu-Kα radiation (λ = 1.5418 Å). Band gap energy analysis was performed using UV-Vis DRS (Agilent Carry 60) at 200-800 nm wavelengths with $BaSO_4$ powder as a blank. The Kubelka Munk equation and the Tauc Plot determined band gap energy values. Functional group analysis was performed using FTIR (Bruker Alpha) in the wavenumber range of 400-4000 cm^{-1}, with a spectral resolution of 4 cm^{-1} and samples prepared in the form of pellets with KBr. Surface morphology was determined using SEM-EDX (JSM 6510) with a voltage of 20 kV.

2.5. Photocatalytic Activity Test of Cu-PTC MOF

A preliminary test was carried out by dispersing 25 mg of Cu-PTC MOF into 50 mL of methylene blue (50 ppm). The mixture was stirred at 300 rpm for 1 hour at room temperature under a visible light source (250-watt mercury lamp) and in the dark (without a light source). Then, 2 mL of the suspension was taken every 15 minutes for 1 hour and centrifuged for 10 minutes at 6000 rpm. The methylene blue concentration was then measured using a UV-Vis spectrophotometer and a standard calibration curve of methylene blue solution at a wavelength of 665 nm. The degradation efficiency and adsorption capacity of methylene blue were calculated using the following equations:

$$\textit{Degradation Efficiency}\ (\%) = \frac{C_0 - C_t}{C_0} \times 100 \quad (1)$$

$$\text{Adsorption Capacity (mg/g)} = \frac{C_0 - C_t}{m} \times V \quad (2)$$

where, C_0 is the initial dye concentration (mg/L), C_t is the dye concentration at a given reaction time (mg/L), m is the mass of the catalyst (g), and V is the volume of the solution (L).

This experiment also determined the optimum conditions for methylene blue degradation by Cu-PTC. The variables studied were methylene blue concentration (25, 50, 75, and 100 ppm), photocatalyst mass (15, 25, 35, and 45 mg), and solution pH (5, 7, and 9).

2.6. Photocatalytic Degradation Kinetics Studies

The optimum condition data were used to study the degradation kinetics using the pseudo-first order and pseudo-second order models, along with the corresponding kinetic equations shown in the following Equations (3)–(4):

$$\ln (C_0/C_t) = kt \quad (3)$$

$$1/C_t = (1/C_0) + k_2 t \quad (4)$$

where, C_0 is the initial dye concentration (mg/L), C_t is the dye concentration at a given reaction time (min), k is the pseudo-first-order rate constant (min^{-1}), and k_2 is the pseudo second-order rate constant (L/mg.min).

3. Results and Discussion

3.1. Cu-PTC Metal Organic Framework (MOF)

In this study, the MOF was synthesized using Cu^{2+} from $(Cu(NO_3)_2.3H_2O)$ as the metal center and PTCDA in its salt form (Na_4PTC) as the organic ligand. Perylene is a carboxylate-type organic ligand that can reduce the bandgap energy of the MOF due to its conjugated aromatic ring system. As a result, incorporating perylene as the ligand enables the resulting MOF to act as a visible-light-responsive photocatalyst [18].

Figure 1 shows the physical appearance of Cu-PTC MOF, which has a dark brown color. The solvothermal method was chosen for synthesizing Cu-PTC MOF because it is straightforward to carry out and capable of producing materials with high crystallinity. The elevated temperature and pressure conditions in this method are particularly suitable for growing crystals with sizes ranging from micrometers to nanometers [21].

Figure 1. Physical appearance of Cu-PTC MOF

3.2. Characteristic of Cu-PTC MOF

3.2.1. Functional group

Figure 2 shows the wavenumber absorption peaks of each functional group in Cu-PTC MOF. When compared with the absorption peaks of Na_4PTC, a shift in wavenumber is observed between the Na_4PTC and Cu-PTC MOF spectra. Table 1 shows that in the FTIR spectrum of Na_4PTC, asymmetric and symmetric stretching vibrations of the carboxylate ion (–COO) appear at wavenumbers 1631 cm^{-1} and 1426 cm^{-1}, respectively, whereas in Cu-PTC MOF, these peaks shift to 1590 cm^{-1} and 1360 cm^{-1}. This shift in wavenumber occurs because the Na-COO bond, which is an ionic bond, being broken and then forming a Cu-COO bond, which is a coordination bond. The coordination bond energy is weaker than the ionic bond energy, causing a shift in the wavenumber towards a smaller value [22].

The FTIR spectrum of Cu-PTC MOF shows an absorption peak at 3450 cm^{-1}, which corresponds to the stretching vibration of the O–H group, likely originating from water molecules or carboxylic acid groups. This absorption peak has also been observed in other copper-based MOFs [23]. The FTIR spectrum of Cu-PTC MOF shows absorption bands at wavenumbers 738 cm^{-1} and 654 cm^{-1}, assigned to the stretching vibrations of the Cu–O group. This is consistent with the findings of Varughese and colleagues, who reported Cu–O stretching vibrations at 784 cm^{-1} and 624 cm^{-1} [24]. Metal–oxygen vibrations typically appear in the wavenumber range of 400–800 cm^{-1} [25]. In addition, an absorption peak at 1689 cm^{-1} is observed, corresponding to the C=O stretching vibration. This may indicate that the carboxylate groups in the PTC ligand coordinate with the metal center in a manner resembling anhydride-like functionality [26]. The FTIR results confirm that Cu-PTC MOF has been successfully synthesized.

3.2.2. Crystallinity and crystal size of Cu-PTC

Based on the diffraction pattern of Cu-PTC (Figure 3), seven distinct peaks with the highest intensities appear at 2θ values of 11.705°, 25.17°, 27.22°, 43.266°, 50.443°, 74.12°, and 89.933°. The crystallinity degree of Cu-PTC MOF is 85.35%, which is significantly higher than that reported by Fathurrahman and colleagues, who obtained a crystallinity degree of 46.56% for Fe-PTC MOF [27]. The crystal size was determined using the Debye–Scherrer equation based on the peak with the highest intensity, yielding a nanoscale crystal size of 35.33 nm for Cu-PTC MOF (Table 2).

The choice of metal can influence the crystal size of MOFs [28]. The crystal size and crystallinity of a MOF photocatalyst can significantly influence its photocatalytic activity. Higher crystallinity generally results in fewer crystal defects. These defects often act as traps for photogenerated electrons and holes,

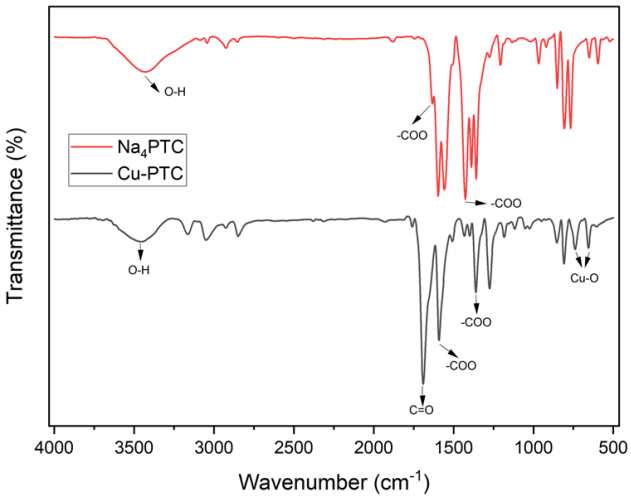

Figure 2. FTIR Spectrum of Na_4PTC and Cu-PTC.

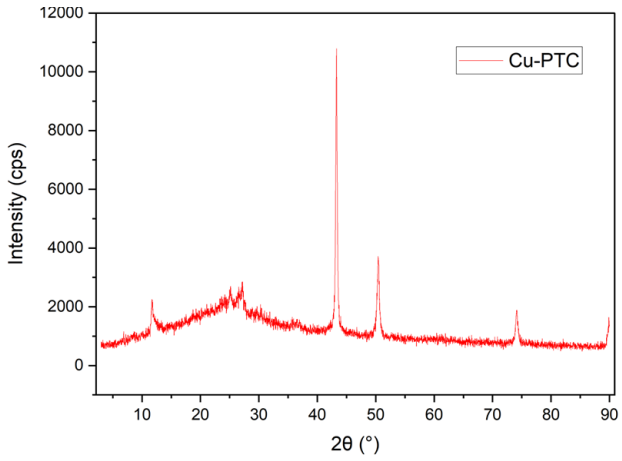

Figure 3. Diffraction pattern of Cu-PTC MOF.

Table 1. Absorption peaks of Na_4PTC and Cu-PTC functional groups.

Wavenumber (cm^{-1})			Description
Na_4PTC	Cu-PTC	Reference	
-	1689	1770 [26]	–C=O stretching
1631	1590	1560 [26]	–COO asymmetric stretching
1426	1360	1355[26]	–COO symmetric stretching
3432	3450	3439 [24]	–OH stretching
-	738, 654	721, 624 [24]	Cu–O stretching

promoting their recombination and thereby reducing photocatalytic efficiency. Conversely, smaller crystal size shortens the migration distance between photogenerated holes (h^+) and electrons (e^-), which decreases the likelihood of recombination and enhances photocatalytic activity [29]. Smaller crystal size leads to a larger specific surface area, which can enhance photocatalytic activity. Conversely, larger crystal size results in a smaller surface area, as a results reducing photocatalytic activity [30].

3.2.3. Band gap energy of Cu-PTC

Figure 4 shows the bandgap energy of Cu-PTC MOF obtained from UV-Vis DRS measurements, which is 1.72 eV. This indicates that Cu-PTC MOF has a narrow bandgap, enabling it to effectively act as a photocatalyst capable of absorbing light in the visible region. The bandgap energy of a material can be influenced by ligands containing conjugated π-bonds and the metal atoms, as reflected in the size of the Secondary Building Unit (SBU). The larger the SBU size of the metal in the framework, the smaller the bandgap energy becomes [31].

The band gap energy value of Cu-PTC is smaller than that of Cu-BTC, wich is based on Cu^{2+} ions and benzene-1,3,5-tricarboxylic acid (H_3BTC) ligands and has a band gap energy of 3.68 eV [32]. The band gap energy of Cu-PTC is smaller than that of Cu-BTC because the PTC ligand possesses a more extended conjugated bond compared to BTC. Additionally, the metal ion also influences the MOF's bandgap energy. For instance, a chromium-based MOF (Cr-PTC) using the same PTC organic ligand has been successfully synthesized and exhibits a higher bandgap energy of 2.01 eV [17]. Fe-PTC MOF has a band gap energy of 1.93 eV [27].

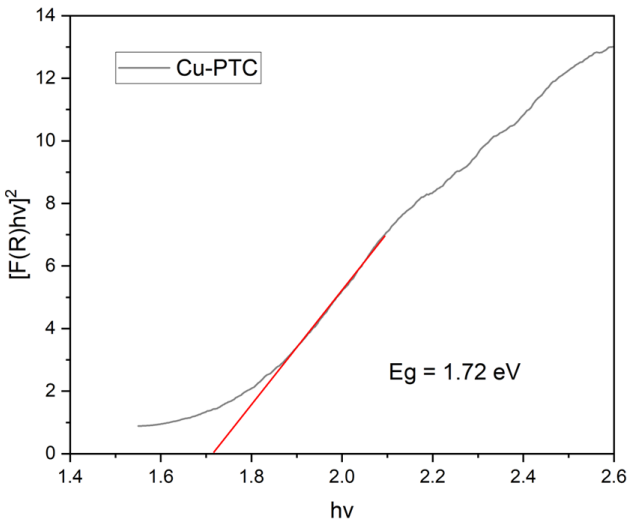

Figure 4. Band gap energy of Cu-PTC.

3.2.4. Morphology of Cu-PTC

The surface morphology analysis of Cu-PTC at magnifications of 1,000x and 10,000x (Figures 5a and 5b) reveals that the particles exhibit a rod-like morphology. Table 3 shows that the elemental composition of Cu-PTC MOF consists of carbon (C), oxygen (O), copper (Cu), and trace impurities, with concentrations of 74.26%, 17.51%, 8.14%, and 0.08%, respectively.

3.3. Photocatalytic Activity of Cu-PTC

Cu-PTC MOF exhibited a methylene blue adsorption percentage of 43.88% under dark conditions after 60 minutes, and a degradation percentage of 71.45% under visible light irradiation (using a mercury lamp) within the same time (Figure 6). The significantly higher degradation percentage under illumination indicates that Cu-PTC possesses photocatalytic activity for the degradation of methylene blue dye.

The photocatalytic process requires the absorption of light at a specific wavelength by a semiconductor material (photocatalyst), which excites electrons from the valence band (VB) to the conduction band (CB). This transition generates positively charged holes (h^+) in the valence band [33]. The photogenerated electrons and positive holes can then migrate to the surface of the photocatalyst and participate in redox reactions

Table 3. Elemental composition of Cu-PTC MOF.

Element	Concentration (%w/w)
C	74.26
O	17.51
Cu	8.14
Impurities	0.08

Table 2. Comparison of diffraction pattern angle and crystal size of Cu-PTC with reference data.

MOF	2θ (°)	Crystal size (nm)
Fe-PTC [27]	9, 12.66, 24.12, 24.88, 25.34, 27.68, 31.74, 33.16, 35.64, 40.88, 45.52, 49.48, 54.06, 57.52, 62.42, 64.02, 71.96	50.9
Cr-PTC [17]	9.17, 12.865, 25.621, 27.85	17.50
Cu-PTC (this study)	11.705, 25.17, 27.22, 43.266, 50.443, 74.12, 89.933	35.33

with adsorbed species, producing superoxide radicals (•O_2^-) and hydroxyl radicals (•OH) [34]. The mechanism for the formation of hydroxyl and superoxide radicals are shown in the following Equations (5)-(8) [35]:

$$\text{MOFs} + h\upsilon \rightarrow \text{MOFs}\,(e^-_{CB} + h^+_{VB}) \quad (5)$$
$$e^- + O_2 \rightarrow \bullet O_2^- \quad (6)$$
$$h^+ + H_2O \rightarrow \bullet OH + H^+ \quad (7)$$
$$\text{Dye} + \bullet OH \rightarrow \text{degradation products} \quad (8)$$

The photocatalytic degradation of methylene blue dye involves hydroxyl radicals (•OH), which attack the N–S heterocyclic group in methylene blue, leading to its cleavage into 2-amino-5-dimethylamino-benzenesulfonic acid anion and N, N-dimethyl-p-phenylenediamine. A series of stepwise oxidations by •OH radicals lead to the formation of simpler aromatic fragments, such as benzenesulfonate derivatives and hydroquinone. This progressive oxidation continues until the carbon backbone is completely decomposed, ultimately yielding CO_2 and H_2O as final products (Figure 7) [36].

3.4. Effect of Methylene Blue Concentration

The degradation efficiencies at methylene blue concentrations of 25, 50, 75, and 100 ppm were 77.53%, 71.45%, 44.55%, and 33.74%, respectively. The optimal methylene blue concentration was determined to be 50 ppm, which corresponded to an adsorption capacity of 73.28 mg/g (Figure 8b). These findings are consistent with the results reported by Saridewi and colleagues, who also identified 50 ppm as the optimal methylene blue concentration for photocatalytic degradation using Cr-PTC [17].

The adsorption capacity at 25 ppm was 38.65 mg/g, which is lower than that at 50 ppm. This is because, at the lower concentration of 25 ppm, fewer methylene blue molecules are available to interact with the active sites of the catalyst, resulting in a lower adsorption capacity compared to the higher concentration. The adsorption capacities at 75 ppm and 100 ppm decreased to 66.62 mg/g and 64.84 mg/g, respectively. This reduction is attributed to the photocatalyst reaching saturation due to the high dye concentration, which leads to excessive coverage of the photocatalyst surface by methylene blue molecules. Once saturated, the photocatalyst experiences reduced photon efficiency and partial deactivation [37].

In general, degradation efficiency decreases as the dye concentration increases. The higher methylene blue concentration leads to greater

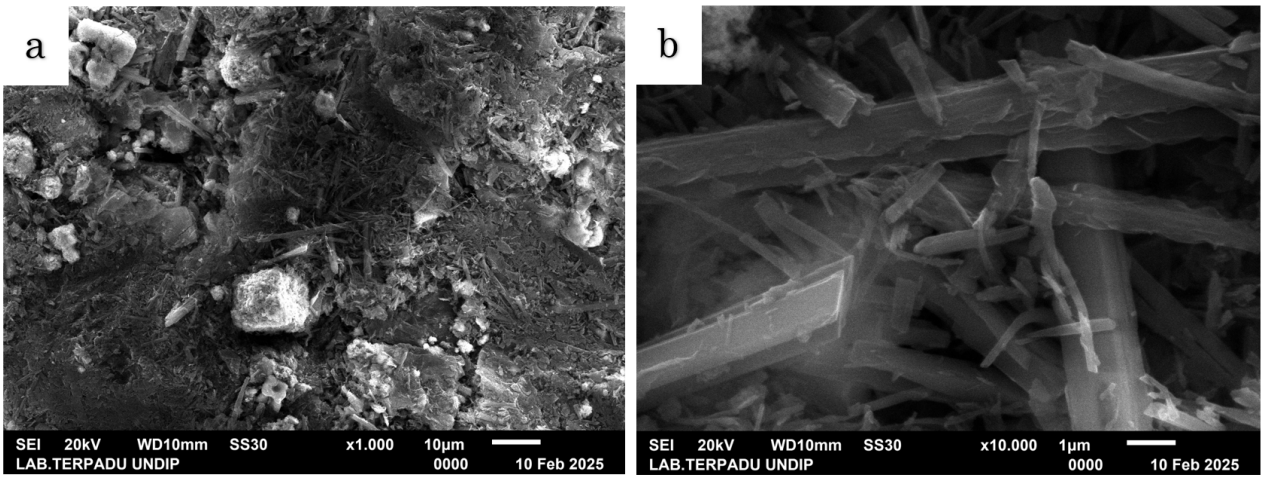

Figure 5. SEM morphology of Cu-PTC MOF (a) 1,000x magnification; (b) 10,000x magnification.

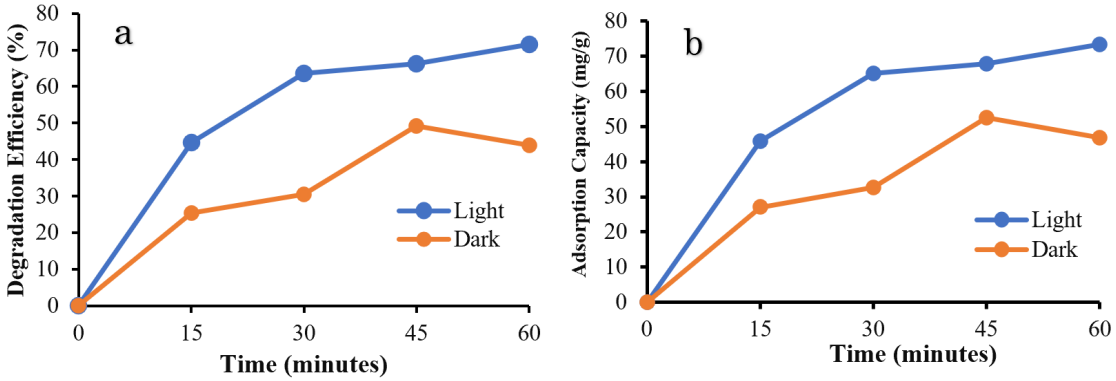

Figure 6. (a) Degradation efficiency, and (b) adsorption capacity of methylene blue in the preliminary test of Cu-PTC.

adsorption of dye molecules onto the photocatalyst surface. This causes the incident light energy to be absorbed or blocked by the excess dye molecules in solution, preventing it from reaching the photocatalyst surface. As a result, the photocatalyst is not effectively irradiated, and electron excitation does not occur. This inhibits the generation of hydroxyl radicals (•OH) and superoxide radicals ($•O_2^-$), which are essential for the degradation of methylene blue [38].

The adsorption capacity of methylene blue using Cu-PTC at a concentration of 50 ppm over 60 minutes is higher than that of Cr-PTC under the same conditions, which yielded approximately 60 mg/g [17]. The degradation efficiency of methylene blue using Cu-PTC at a concentration of 50 ppm within 15 minutes was 44.63%, which is higher than that of Cu-BTC, which achieved only 32.4% degradation efficiency at a lower MB concentration of 30 ppm under the same irradiation time [39].

3.5. Effect of Cu-PTC Mass

The results show that increasing the mass of Cu-PTC MOF leads to higher degradation percentages (Figure 9a). Specifically, Cu-PTC masses of 15, 25, 35, and 45 mg yielded degradation efficiencies of 42.38%, 71.45%, 72.35%, and 88.03%, respectively. This trend is consistent with the study by Lubis and colleagues, who reported that higher photocatalyst loading results in greater degradation efficiency [40]. The increase in photocatalyst amount is associated with a greater number of active surface sites, which enhances the generation of hydroxyl radicals that play a key role in degrading the dye [38].

A Cu-PTC mass of 25 mg was identified as the optimal dosage, yielding the highest adsorption capacity of 73.28 mg/g. In comparison, MOF masses of 15, 35, and 45 mg resulted in adsorption capacities of 71.24, 51.63, and 47.67 mg/g, respectively (Figure 9b). The decrease in adsorption capacity at 35 mg and 45 mg is attributed to increased turbidity in the solution caused by the excessive amount of photocatalyst. This high catalyst loading enhances light scattering and reduces light penetration depth, thereby limiting photon availability for photocatalytic activation and ultimately lowering adsorption performance [41].

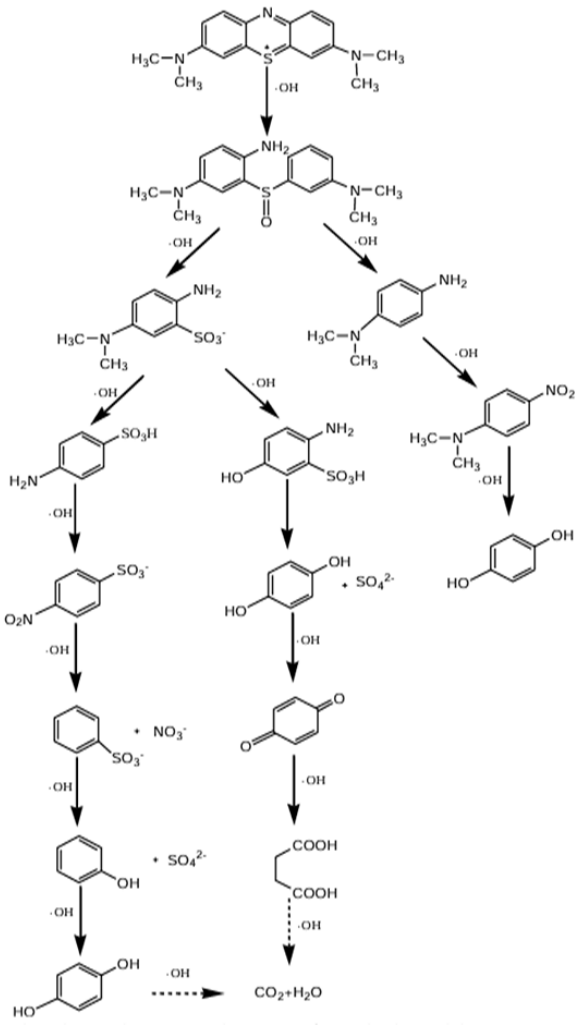

Figure 7. Degradation mechanism of methylene blue dye.

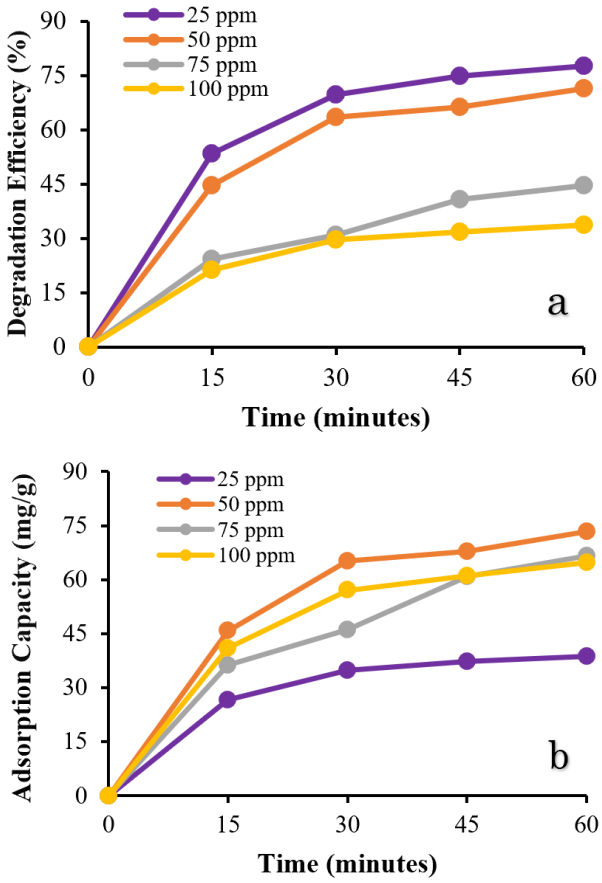

Figure 8. (a) Degradation efficiency, and (b) adsorption capacity at varying concentrations of methylene blue.

3.6. Effect of pH

The results of the pH variation test in the methylene blue degradation process by Cu-PTC MOF are shown in Figures 10a and 10b. The degradation efficiency of Cu-PTC MOF at pH of 5 yielded a degradation percentage of 9.78%. The degradation efficiency of Cu-PTC MOF at pH of 7 gave the highest degradation efficiency of 71.45%, while at pH of 9, its degradation efficiency was 67.58%. At pH of 5, there was no photocatalytic activity due to the absence of a significant increase in degradation efficiency. At pH of 7 and 9, high degradation efficiencies were observed, indicating the presence of photocatalytic activity under these conditions. pH of 7 exhibited the highest adsorption capacity, at 73.28 mg/g, while pH of 5 and pH of 9 showed adsorption capacities of 10.48 mg/g and 66.68 mg/g, respectively. Based on these results, pH of 7 represents the optimal condition for the photocatalytic activity of Cu-PTC.

The pH condition can influence the photocatalytic activity of a photocatalyst. Under acidic conditions, H^+ ions interact with carboxylate groups, resulting in a positively charged catalyst surface. In contrast, under basic conditions, OH^- ions interact with hydrogen atoms on the organic ligand, leading to a negatively charged surface [18]. For that reason, under acidic conditions, the positively charged surface of Cu-PTC experiences repulsion with the cationic methylene blue dye molecules, reducing dye adsorption onto the MOF surface and consequently decreasing degradation efficiency. A similar result was reported by Saridewi and colleagues, who used Cr-PTC for methylene blue photodegradation and observed no significant increase in degradation efficiency at pH of 5 [17].

Under basic conditions, the surface of Cu-PTC MOF becomes negatively charged, causing attractive forces with the cationic methylene blue dye molecules. This leads to increased adsorption of the dye onto the MOF surface, and degradation efficiency also increases under basic conditions compared to acidic conditions. However, at pH of 9, the degradation efficiency was lower than that at pH of 7. This is consistent with the study by Suprihatin and colleagues, who found that the

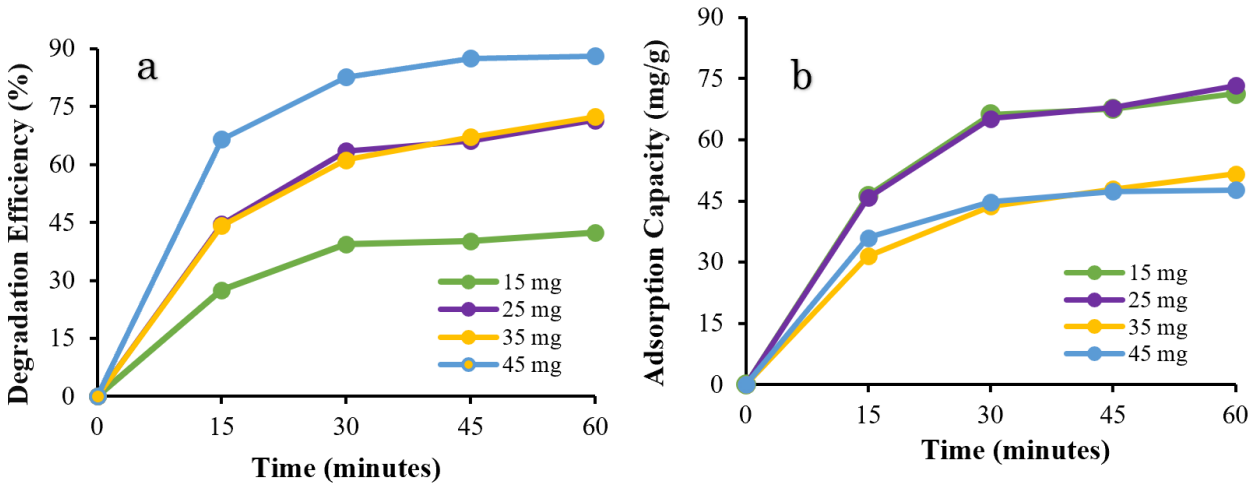

Figure 9. (a) Degradation efficiency, and (b) adsorption capacity of methylene blue at varying masses of Cu-PTC.

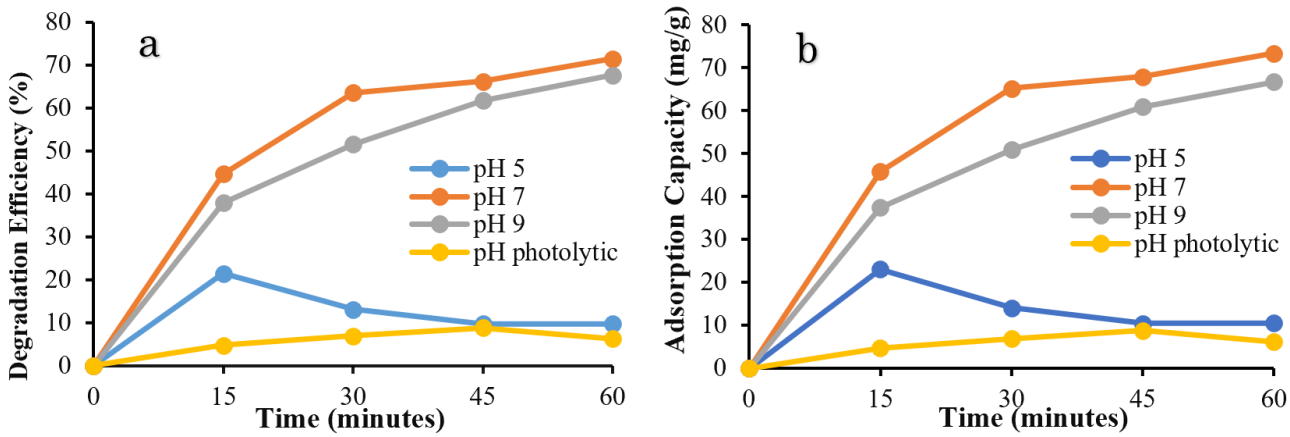

Figure 10. (a) Degradation efficiency, and (b) adsorption capacity of methylene blue at varying solution pH levels.

more basic the solution, the lower the degradation efficiency. This is likely due to excess OH^- ions covering the photocatalyst surface, causing strong adsorption of positively charged methylene blue molecules onto the photocatalyst. As a result, the photocatalyst surface becomes blocked by methylene blue molecules, leading to suboptimal light absorption and reduced generation of free radicals available for degrading methylene blue [42].

Figure 10a shows that the degradation efficiency of methylene blue with the addition of Cu-PTC is significantly higher than that without a photocatalyst. This demonstrates that the addition of Cu-PTC photocatalyst substantially enhances the degradation rate. The presence of the photocatalyst increases the degradation rate due to the generation of free radical species, which play a crucial role in the degradation process.

3.7. Degradation Kinetics of Cu-PTC towards Methylene Blue

A degradation kinetics plot was constructed to determine the kinetic parameters of Cu-PTC in degrading methylene blue. Figure 11 shows presents the degradation kinetics of methylene blue fitted to both pseudo first-order and pseudo second- order models. The correlation coefficient (R^2) for the pseudo second-order model (0.9579) is higher than of the pseudo first-order model (0.8885). This indicates that the degradation rate follows pseudo second-order kinetics.

4. Conclusions

The synthesis of Cu-PTC MOFs yielded a narrow bandgap energy of 1.72 eV. The FTIR spectrum of Cu-PTC MOF shows characteristic functional groups at wavenumbers 1689 cm^{-1} (C=O), 1590 and 1360 cm^{-1} (-COO), 3450 cm^{-1} (OH), 738 and 654 cm^{-1} (Cu-O). The diffraction patterns of Cu-PTC MOFs with 2θ angles of 11.705°, 25.17°, 27.22°, 43.266°, 50.443°, 74.12°, and 89.933°, with a crystallinity degree of 85.35% and a crystallite size of 35.33 nm, and a rod-like surface morphology. Cu-PTC MOF demonstrates photocatalytic activity in degrading methylene blue dye under visible light irradiation, achieving a degradation efficiency of 71.45% and an adsorption capacity of 73.28 mg/g under optimal conditions: 50 mL of 50 ppm methylene blue solution, 25 mg of Cu-PTC MOF, and pH of 7. Reusability testing and radical trapping experiments are required to evaluate the stability of Cu-PTC MOF and to identify the reactive species involved in the photocatalytic degradation mechanism of methylene blue.

Acknowledgment

The authors would like to express their gratitude to Integrated Laboratory Centre (PLT) UIN Syarif Hidayatullah Jakarta for facilitating this work.

CRedit Author Statement

Author Contributions: F. S. Mala: formal analysis, investigation, data gathering, writing an original draft; N. Saridewi: conceptualization, validation, resources, review; S. Nurbayti: Supervision, oversaw writing; Adawiah: Supervision, data curation, reviewing; A. Zulys: Supervision, resources. All authors have read and agreed to the published version of the manuscript.

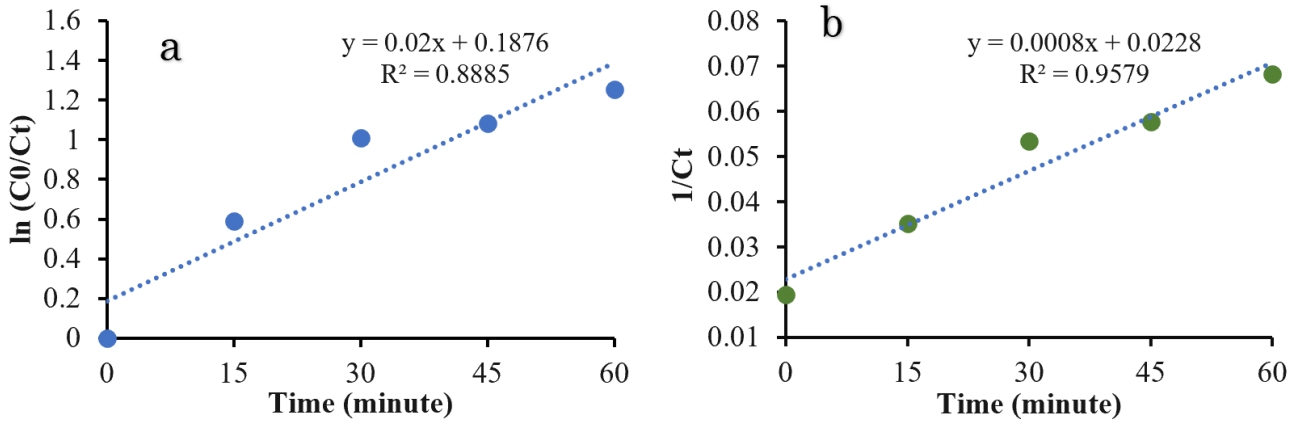

Figure 11. (a) Plots of pseudo first-order model (k = 0.02 min^{-1}; R^2 = 0.8885), and (b) pseudo second-order model (k_2 = 0.0008 L/mg.min; R^2 = 0.9579) for methylene blue degradation.

References

[1] Rather, L.J., Akhter, S., Hassan, Q.P. (2018). Bioremediation: Green and Sustainable Technology for Textile Effluent Treatment. In: Muthu, S. (eds) *Sustainable Innovations in Textile Chemistry and Dyes*. Singapore: Springer.

[2] Hassani, A., Eghbali, P., Metin, Ö. (2018). Sonocatalytic Removal of Methylene Blue from Water Solution by Cobalt Nanocomposites : Response Surface Methodology Approach. *Environmental Science and Pollution Research*, *25*(32), 32140-32155. DOI: 10.1007/s11356-018-3151-3.

[3] Oladoye, P.O., Ajiboye, T.O., Omotola, E.O., Oyewola, O.J. (2022). Methylene Blue Dye: Toxicity and Potential Elimination Technology from Wastewater. *Results in Engineering*, 16 (August), 100678. DOI: 10.1016/j.rineng.2022.100678.

[4] Paździor, K., Bilińska, L., Ledakowicz, S. (2018). A Review of the Existing and Emerging Technologies in the Combination of AOPs and Biological Processes in Industrial Textile Wastewater Treatment. *Chem. Eng. J.* 376 (15 November), 120597. DOI: 10.1016/j.cej.2018.12.057

[5] Martinez-Huitle, C.A., Rodrigo, M.A., Sires, I., Scialdone, O. (2015). Single and Coupled Electrochemical Processes and Reactors for the Abatement of Organic Water Pollutants : A Critical Review. *Chemical reviews*, *115*(24), 13362-13407. DOI: 10.1021/acs.chemrev.5b00361

[6] Hassani, A., Pourshirband, N., Sayyar, Z., Eghbali, P. (2025). Fenton and Fenton-like-based Advanced Oxidation Processes. In *Innovative and Hybrid Advanced Oxidation Processes for Water Treatment* (pp. 171-203). Elsevier. DOI: 10.1016/B978-0-443-14100-3.00006-5.

[7] Brillas, E., Martínez-Huitle, C.A. (2014). Decontamination of Wastewaters Containing Synthetic Organic Dyes by Electrochemical Methods. An updated review. *Applied Catalysis B: Environmental*, *166*, 603-643. DOI: 10.1016/j.apcatb.2014.11.016

[8] Ghorbani, P., Hassani, A., Eghbali, P., Abbasi, A. (2025). Activated Carbon-Based Photocatalysts for the Removal of Pesticides. *Pesticide Removal Methods from Wastewater: Proactive Approaches and Future Trends*, 203. DOI: 10.1201/9781779641212-7.

[9] Annisaputri, W., Azzah, A., Wibisono, R. (2020). Studi Potensi Fotokatalis dari Material Kerangka Logam-Organik (Metal-Organic Framework) untuk Degradasi Zat Pewarna Limbah Batik. *The Indonesian Green Technology Journal*, 42–53. DOI: 10.21776/ub.igtj.2020.009.02.03.

[10] Natarajan, S., Bajaj, H.C., Tayade, R.J. (2018). Recent Advances Based on the Synergetic Effect of Adsorption for Removal of Dyes from Waste Water using Photocatalytic Process. *Journal of Environmental Sciences (China)*, 65, 201–222. DOI: 10.1016/j.jes.2017.03.011.

[11] Wang, C.C., Li, J.R., Lv, X.L., Zhang, Y.Q., Guo, G. (2014). Photocatalytic Organic Pollutants Degradation in Metal-Organic Frameworks. *Energy and Environmental Science*, 7(9), 2831–2867. DOI: 10.1039/c4ee01299b.

[12] Zhang, Y.-B., Furukawa, H., Ko, N., Nie, W., Park, H.J., Okajima, S., Cordova, K.E., Deng, H., Kim, J., Yaghi, O.M. (2015). Introduction of Functionality, Selection of Topology, and Enhancement of Gas Adsorption in Multivariate Metal–Organic Framework-177. *Journal of the American Chemical Society*, 137(7), 2641–2650. DOI: 10.1021/ja512311a.

[13] Li, M., Li, D., O'Keeffe, M., Yaghi, O.M. (2014). Topological Analysis of Metal–Organic Frameworks with Polytopic Linkers and/or Multiple Building Units and the Minimal Transitivity Principle. *Chemical Reviews*, 114(2), 1343–1370. DOI: 10.1021/cr400392k.

[14] Syaima, H., Kumalasari, M.R., Hanif, Q.A., Hiyahara, I.A., Salsabila, A.P., Zahra, M.A. (2024). Photocatalytic Potential of Metal-Organic Frameworks for Pollutant Degradation: A Literature Review. *Evergreen*, 11(3), 1715–1731. DOI: 10.5109/7236824.

[15] Abdelhamid, H.N. (2017). Lanthanide Metal-Organic Frameworks and Hierarchical Porous Zeolitic Imidazolate Frameworks: Synthesis, Properties, and Applications. *Ph.D. Dissertation*, Department of Materials and Environmental Chemistry, Stockholm University.

[16] Mahreni, Ristianingsih, Y., Suhascaryo, N. (2020). *Sintesis dan Aplikasi Material Baru Kerangka Logam Organik (Metal Organic Framework, MOF)*. Yogyakarta: Universitas Pembangunan Nasional "Veteran".

[17] Saridewi, N., Azhar, F.M., Abdillah, P.A., Zulys, A., Nurbayti, S., Tulhusna, L., Adawiah, A. (2022). Synthesize Metal-Organic Frameworks From Chromium Metal Ions and PTCDA Ligands for Methylene Blue Photodegradation. *Rasayan Journal of Chemistry*, 15(4), 2544–2550. DOI: 10.31788/RJC.2022.1547046.

[18] Yuan, S., Feng, L., Wang, K., Pang, J., Bosch, M., Lollar, C., Sun, Y., Qin, J., Yang, X., Zhang, P., Wang, Q., Zou, L., Zhang, Y., Zhang, L., Fang, Y., Li, J., Zhou, H.C. (2018). Stable Metal–Organic Frameworks: Design, Synthesis, and Applications. *Advanced Materials*, 30(37). DOI: 10.1002/adma.201704303.

[19] Zhang, M., Wang, L., Zeng, T., Shang, Q., Zhou, H., Pan, Z., Cheng, Q. (2018). Two Pure MOF-photocatalysts Readily Prepared for the Degradation of Methylene Mlue Dye Under Visible Light. *Dalton Transactions*, 47(12), 4251–4258. DOI: 10.1039/C8DT00156A.

[20] Haso, H.W., Dubale, A.A., Chimdesa, M.A., Atlabachew, M. (2022). High Performance Copper Based Metal Organic Framework for Removal of Heavy Metals From Wastewater. *Frontiers in Materials*, 9(March), 1–11. DOI: 10.3389/fmats.2022.840806.

[21] Ningsih, S.K.W. (2016). *Sintesis Anorganik*. Padang: UNP Press Padang.

[22] Shen, Z., He, S., Yao, P., Lao, X., Yang, B., Dai, Y., Sun, X., Chen, T. (2014). Lanthanum-based Coordination Polymers Microplates using a "Green Ligand" EDTA with Tailorable Morphology and Fluorescent Property. *RSC Advances*, 4(25), 12844–12848. DOI: 10.1039/c3ra46829a.

[23] Salama, R.S., Abd El-Hakam, S., Elsayed Samra, S., El-dafrawy, S.M., El-Hakam, S.A., Samra, S.E., El-Dafrawy, S.M., Ahmed, A.I. (2018). Adsorption, Equilibrium and kinetic studies on the removal of methyl orange dye from aqueous solution by the use of copper metal organic framework (Cu-BDC). *International Journal of Modern Chemistry*, 10(2), 195–207.

[24] Varughese, A., Kaur, R., Singh, P. (2020). Green Synthesis and Characterization of Copper Oxide Nanoparticles Using Psidium guajava Leaf Extract. *IOP Conference Series: Materials Science and Engineering*, 961(1), 012011. DOI: 10.1088/1757-899X/961/1/012011.

[25] Shadmehr, J., Zeinali, S., Tohidi, M. (2019). Synthesis of a Chromium Terephthalate Metal Organic Framework and use as Nanoporous Adsorbent for Removal of Diazinon Organophosphorus Insecticide from Aqueous Media. *Journal of Dispersion Science and Technology*, 40(10), 1423–1440. DOI: 10.1080/01932691.2018.1516149.

[26] Christina, L.C., Gunlazuardi, J., Zulys, A. (2020). Synthesis and Characterization of Lanthanide Metal-Organic Framework with Perylene 3,4,9,10-tetracarboxylate Ligand. *IOP Conference Series: Materials Science and Engineering*, 902(1) DOI: 10.1088/1757-899X/902/1/012046.

[27] Fathurrahman, M., Zulys, A., Gunlazuardi, J. (2024). Fotodegradasi Metilen Biru oleh Metal Organic Framework (MOF) Fe-PTC dengan Penambahan H_2O_2 dan Dioptimasi Menggunakan Desain Box Behnken. *Jurnal Kartika Kimia*, 6(11), 131–144. DOI: 10.26874/jkk.v6i2.228.

[28] Ban, Y., Li, Y., Liu, X., Peng, Y., Yang, W. (2013). Solvothermal Synthesis of Mixed-ligand Metal-Organic Framework ZIF-78 with Controllable Size and Morphology. *Microporous and Mesoporous Materials*, 173, 29–36. DOI: 10.1016/j.micromeso.2013.01.031.

[29] Kudo, A., Miseki, Y. (2009). Heterogeneous Photocatalyst Materials for Water Splitting. *Chemical Society Reviews*, 38(1), 253–278. DOI: 10.1039/b800489g.

[30] Rosanti, A.D., Wardani, A.R.., Latifah, E.U. (2020). Pengaruh Variasi Konsentrasi Urea Terhadap Fotoaktivitas Material Fotokatalis N/TiO2 Untuk Penjernihan Limbah Batik Tenun Ikat Kediri. *Jurnal Kimia Riset*, 5(1), 55. DOI: 10.20473/jkr.v5i1.18169.

[31] Lin, C.K., Zhao, D., Gao, W.Y., Yang, Z., Ye, J., Xu, T., Ge, Q., Ma, S., Liu, D.J. (2012). Tunability of Band Gaps in Metal-Organic Frameworks. *Inorganic Chemistry*, 51(16), 9039–9044. DOI: 10.1021/ic301189m.

[32] Samuel, M.S., Savunthari, K.V., Ethiraj, S. (2021). Synthesis of a Copper (II) Metal–Organic Framework for Photocatalytic Degradation of Rhodamine B Dye in Water. *Environmental Science and Pollution Research*, 28(30), 40835–40843. DOI: 10.1007/s11356-021-13571-9.

[33] Li, Y., Fu, Y., Zhu, M. (2020). Green Synthesis of 3D Tripyramid TiO2 Architectures with Assistance of Aloe Extracts for Highly Efficient Photocatalytic Degradation of Antibiotic Ciprofloxacin. *Applied Catalysis B: Environmental*, 260, 118149. DOI: 10.1016/j.apcatb.2019.118149.

[34] Romeiro, A., Freitas, D., Emília Azenha, M., Canle, M., Burrows, H.D. (2017). Effect of the Calcination Temperature on the Photocatalytic Efficiency of Acidic Sol–gel Synthesized TiO_2 Nanoparticles in the Degradation of Alprazolam. *Photochemical & Photobiological Sciences*, 16(6), 935–945. DOI: 10.1039/c6pp00447d.

[35] Liu, Y., Liu, Z., Huang, D., Cheng, M., Zeng, G., Lai, C., Zhang, C., Zhou, C., Wang, W., Jiang, D., Wang, H., Shao, B. (2019). Metal or Metal-containing Nanoparticle@MOF Nanocomposites as a Promising Type of Photocatalyst. *Coordination Chemistry Reviews*, 388, 63–78. DOI: 10.1016/j.ccr.2019.02.031.

[36] Wang, X.Q., Han, S.F., Zhang, Q.W., Zhang, N., Zhao, D.D. (2018). Photocatalytic Oxidation Degradation Mechanism Study of Methylene Blue Dye Waste Water with GR/iTO_2. *MATEC Web of Conferences*, 238 DOI: 10.1051/matecconf/201823803006.

[37] Chen, X., Mao, S.S. (2007). Titanium Dioxide Nanomaterials: Synthesis, Properties, Modifications and Applications. *Chemical Reviews*, 107(7), 2891–2959. DOI: 10.1021/cr0500535.

[38] Kumar, A. (2017). A Review on the Factors Affecting the Photocatalytic Degradation of Hazardous Materials. *Material Science & Engineering International Journal*, 1(3). DOI: 10.15406/mseij.2017.01.00018.

[39] Aziz, D.M., Hassan, S.A., Aziz, S.B., Kader, D.A. (2025). Efficient Adsorption and Photocatalytic Degradation of Methylene Blue using HKUST-1: A Novel Approach for Dye Removal and Wastewater Treatment under Sunlight. *Next Materials*, 9(April), 101015. DOI: 10.1016/j.nxmate.2025.101015.

[40] Lubis, S., Sheilatina, Wardani Sitompul, D. (2019). Photocatalytic Degradation of Indigo Carmine Dye using α-Fe_2O_3 /Bentonite Nanocomposite Prepared by Mechanochemical Synthesis. *IOP Conference Series: Materials Science and Engineering*, 509(1), 012142. DOI: 10.1088/1757-899X/509/1/012142.

[41] Khan, S., Noor, T., Iqbal, N., Yaqoob, L. (2024). Photocatalytic Dye Degradation from Textile Wastewater: A Review. *ACS Omega*, 9(20), 21751–21767. DOI: 10.1021/acsomega.4c00887.

[42] Suprihatin, I.E., Suat, R.M., Negara, I.M.S. (2022). Fotodegradasi Zat Warna Methylene Blue Dengan Sinar UV Dan Fotokatalis Nanopartikel Perak. *Jurnal Kimia*, 16(2), 168. DOI: 10.24843/jchem.2022.v16.i02.p06.